ELSEVIER

Journal of Alloys and Compounds 356–357 (2003) 429–432

Journal of ALLOYS AND COMPOUNDS

www.elsevier.com/locate/jallcom

Hydriding properties of ordered-/disordered-Mg-based ternary Laves phase structures

Nobuko Hanada*, Shin-ichi Orimo, Hironobu Fujii

Faculty of Integrated Arts and Sciences, Hiroshima University, Higashi-Hiroshima 739-8521, Japan

Received 10 June 2002; received in revised form 8 January 2003; accepted 15 January 2003

Abstract

Ternary Laves phase structures with compositions $MgYNi_4$, $MgCaNi_4$ and $CaYNi_4$ were prepared, and the relationship between the structures and hydriding properties was studied in detail. Only in $MgYNi_4$ are Mg and Y found to be ordered and a plateau pressure is clearly observed in the *P–C* isotherm during the dehydriding process. In $MgCaNi_4$, however, Mg and Ca are disordered, and hydrogen content of $MgCaNi_4$ is ~30% larger than that of $MgYNi_4$. Control of their order/disorder in Laves phase structures may provide the hydriding properties with higher hydrogen concentrations and flatter plateau regions.

Keywords: Hydrogen storage material; Mechanical alloying; X-ray diffraction; Thermal analysis

1. Introduction

The structural and hydriding properties of the Mg-based alloys have been extensively investigated as regards their effective use as functional materials for hydrogen storage and transportation. In the binary Mg-based system, we have so far investigated the hydriding properties of nano-structured- and amorphous-structured Mg–Ni [1,2]. In the ternary system, Tsushio and Akiba have systematically studied the hydriding properties of $Mg(Ni_{1.9}M_{0.1})$ (M=Cr, Mn, Fe) with the AB_2-type Laves phase structure [3,4], and Oesterreicher et al. have reported the hydriding properties of $(Mg_xR_{1-x})Ni_2$ (x=0−1.0, R=Ca, La) [5,6]. Kohno et al. and Terashita et al. have also studied the hydriding properties of Mg–La–Ni system [7] and $Mg_{1-x}Ca_xNi_2$ (x=0–1.0) [8], respectively.

Recently we have focused on the ternary compound $MgRNi_4$ with the C15*b*($AuBe_5$)-type Laves phase structure reported by Geibel et al. for R=Ce [9] and Kadir et al. for R=Ca, La, Ce, Pr, Nd and Y [10], and have examined the hydriding properties of $MgYNi_4$ [2,11]. $MgYNi_4$ is located at the middle point between $MgNi_2$ with the C36($MgNi_2$)-type Laves phase structure, and YNi_2 with a modification C15($MgCu_2$)-type Laves phase structure which is crystallized in a superstructure with ordered vacancies [12]. $MgNi_2$ does not react with hydrogen at the crystalline state [13], while YNi_2 transforms into an amorphous phase upon hydrogenation, which is known as hydrogen induced amorphization (HIA) [14–18].

In this work, we paid attention to $CaNi_2$ with the C15($MgCu_2$)-type Laves phase structure [5]. By mechanically milling two of three binary Laves phase compounds ($MgNi_2$, YNi_2, $CaNi_2$), some new Laves phase compounds, $MgYNi_4$, $MgCaNi_4$ and $CaYNi_4$, were prepared and the relationships between the structures and hydriding properties were studied in detail.

2. Experimental procedures

Mechanical milling was employed for the sample preparation of $MgYNi_4$, $MgCaNi_4$, and $CaYNi_4$. The starting materials were $MgNi_2$ and $CaNi_2$ prepared by r.f. induction-melting, and YNi_2 prepared by arc-melting. The mixtures of the starting materials were put into a chrome steel vial (3×10^{-5} m^3 volume) together with 20 chrome steel balls (7 mm in diameter, mass ratio 1:30). Then the vial was degassed below 0.01 Pa for 12 h. After introduction of high-purity argon (7 N) at 1.0 MPa, the mixtures were mechanically milled for 80 h using a planetary ball apparatus (Fritsch P7, 400 rpm). Parts of

*Corresponding author.
E-mail address: hanadan@hiroshima-u.ac.jp (N. Hanada).

0925-8388/03/$ – see front matter
doi:10.1016/S0925-8388(03)00227-5

samples were then heated up to 773 K. After milling, vials were degassed and all samples were hydrogenated under high-purity hydrogen (7 N) at 2.0 MPa. All samples were handled in a glove box filled with purified argon (oxygen density below 1 ppm, the dew point below 185 K).

The structural properties and lattice parameter were examined by X-ray diffraction measurement (Rigaku RINT2000, Cu Kα). The lattice parameter was calculated from the peak position of X-ray diffraction profiles. The hydrogen content and dehydriding properties were examined by thermal analysis (Seiko TG/DTA300), under a high-purity argon atmosphere with heating rate of 5 K min^{-1} up to 773 K.

3. Results and discussion

Fig. 1 shows the X-ray diffraction profiles of samples heat-treated at 773 K after the mechanical milling.

In Fig. 1(a), both the 200 and 420 diffraction peaks for $MgYNi_4$ corresponding to the elementally ordered lattice peaks are clearly observed, indicating the formation of the C15*b*($AuBe_5$)-type Laves phase structure which is schematically shown in Fig. 2. The diffraction peak positions and their intensities are in good agreement with that after simulation under an assumption of full-ordering of Mg and Y (Fig. 1(b)). The lattice parameter was estimated to be $a=0.701$ nm.

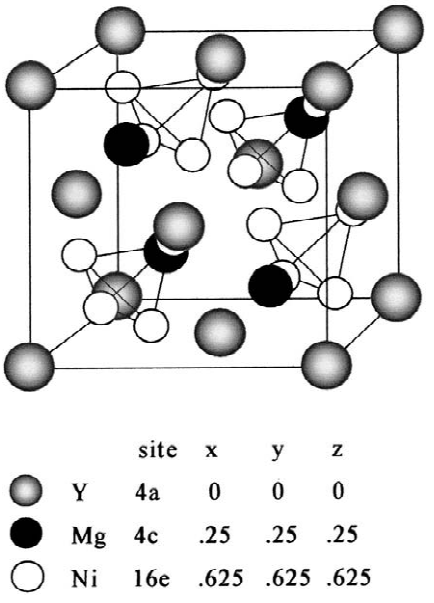

Fig. 2. Atomic structure of $MgYNi_4$ with the C15*b*-type Laves phase structure.

The ordered process with heat-treatment up to 773 K after milling was estimated by differential thermal analysis (DTA), which is shown in Fig. 3. A broad exothermic peak appears around 600 K. The X-ray diffraction profiles before and after this exothermic peak are shown in Fig. 4. The diffraction peaks just after milling are broad, indicating the formation of nanometer-scale grains and lattice strains. Up to 526 K just before the exothermic peak, the diffraction profile hardly changes. At 653 K after the exothermic peak, the diffraction peaks become rather sharp and the ordered lattice peak 200 appears. Therefore, this

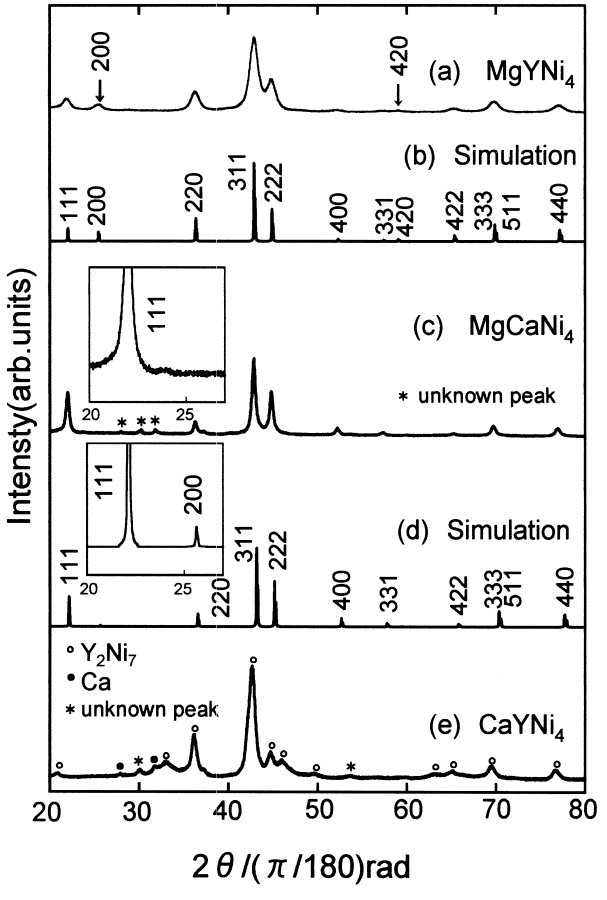

Fig. 1. X-ray diffraction profiles of (a) $MgYNi_4$ and (b) its simulation, (c) $MgCaNi_4$ and (d) its simulation, and (e) $CaYNi_4$. The samples were heat-treated at 773 K after mechanical milling for 80 h.

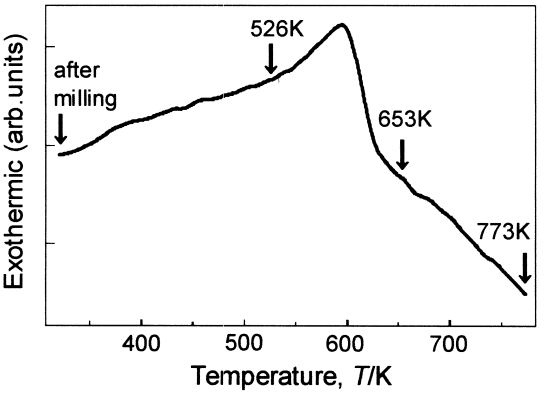

Fig. 3. Differential thermal analysis (DTA) of $MgYNi_4$ after milling for 80 h.

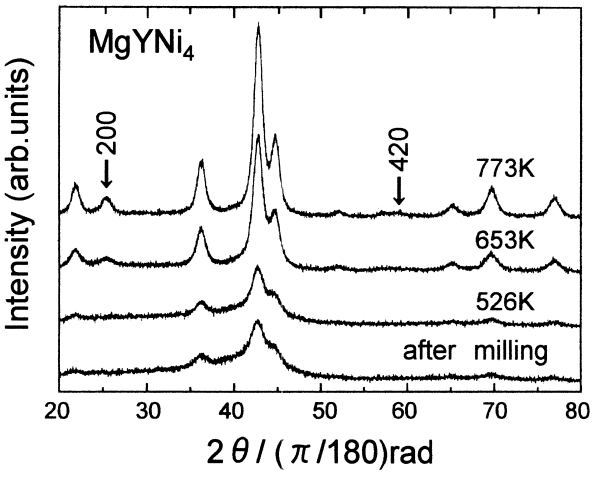

Fig. 4. X-ray diffraction profiles of $MgYNi_4$ after milling and heating up to 773 K.

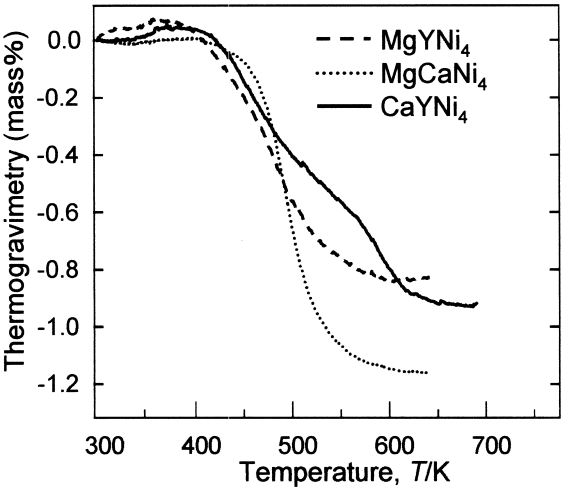

Fig. 5. Thermogravimetric (TG) profiles of the hydrogenated $MgYNi_4$, $MgCaNi_4$ and $CaYNi_4$.

exothermic peak is caused by the grain growth and ordering of elemental Mg and Y in the long distance.

In Fig. 1(c), the diffraction peaks for $MgCaNi_4$ corresponding to the C15($MgCu_2$)-type Laves phase structure are observed with a small amount of precipitated unknown phases. Neither the 200 nor the 420 diffraction peak can be observed at all, although the intensity of the 200 diffraction peak is found to be only one twenty-fifth after simulation under an assumption of full-ordering of Mg and Ca (Fig. 1(d)). Therefore, the elemental Mg and Ca atoms do not fully order, and the C15($MgCu_2$)-type Laves phase structure is formed. The lattice parameter was estimated to be $a=0.701$ nm, just the same as that for $MgYNi_4$.

Finally, in $CaYNi_4$ (Fig. 1(e)), there are multi phases of Y_2Ni_7, Ca and a small amount of precipitated phases. Since elements of Ca and Y do not have any affinity, it is not realized to form the single phased ternaries.

Thermogravimetry (TG) profiles of the three hydrogenated samples are shown in Fig. 5. For all the samples, the dehydrogenation reaction starts around 400 K. Both $MgYNi_4$ and $MgCaNi_4$ have one dehydrogenation reaction, while $CaYNi_4$ has two dehydrogenation reactions around 400 and 600 K, arising from the formation of multi phases.

The hydrogen content of $MgYNi_4$ is estimated to be 0.92 mass% (H/M=0.53), while that of $MgCaNi_4$ is ~30% larger than that of $MgYNi_4$, 1.18 mass% (H/M= 0.59). The different hydrogen contents might be dominantly coming from the ordering or disordering properties of their structures, because both lattice parameters are the same: $a=0.701$ nm.

In the hydrogen pressure–composition (P–C) isotherms in the dehydriding process of $MgYNi_4$ synthesized by casting, a flat plateau (miscibility-gap) pressure was clearly observed around room temperature, as shown in Fig. 6 [2,11]. This property is caused by the ordering of elemental Mg and Y atoms. In other words, the tetrahedral site composed of [1Mg1Y2Ni] is preferably formed, and thus the energy level of hydrogen atom in the tetrahedral site become homogeneous. On the other hand, in the P–C isotherms of $(Mg_{0.56}Ca_{0.44})Ni_2$, a sloping plateau pressure was observed [8], which is due to the variation of the energy level of hydrogen atoms locating in the tetrahedral sites composed of [2Mg2Ni], [2Ca2Ni] and [1Mg1Ca2Ni].

4. Conclusion

The relationships between the structural and hydriding properties were studied on ternary Laves phase structures. In $MgYNi_4$, the C15b($AuBe_5$)-type Laves phase structure ordering elemental Mg and Y atoms is formed, while the C15($MgCu_2$)-type Laves phase structure with disordering elemental Mg and Ca atoms is formed in $MgCaNi_4$. Multi phases were formed in $CaYNi_4$. Although both lattice

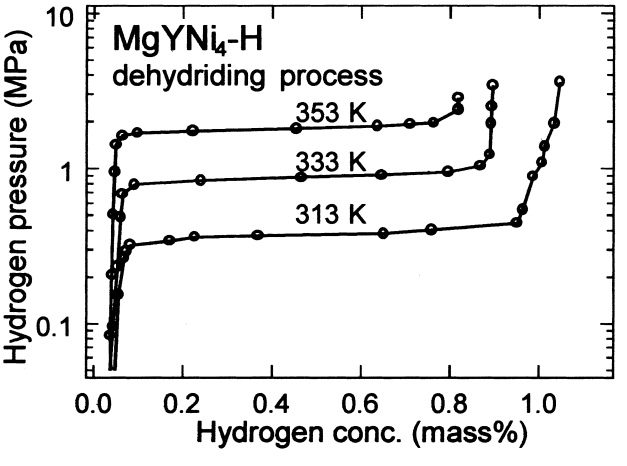

Fig. 6. Hydrogen pressure–composition (P–C) isotherm of $MgYNi_4$-H synthesized by casting [2,11].

parameters are almost the same, the hydrogen content in $MgCaNi_4$ was 30% larger than that in $MgYNi_4$. Only in the case of $MgYNi_4$ is a flat plateau pressure clearly observed in the $P–C$ isotherm for the dehydriding process. Hence the atomic ordering or disordering properties in the Laves phase structures might dominantly affect the flatness of the $P–C$ isotherms. Control of their order/disorder may provide the hydriding properties with higher hydrogen concentrations and flatter plateau regions.

Acknowledgements

This work was partially supported by a Ministry of Education, Science, Sports and Culture, Grant-in-Aid for Scientific Research on Priority Area and on COE (13CE202).

References

[1] S. Orimo, H. Fujii, Intermetallics 6 (1998) 185.
[2] S. Orimo, H. Fujii, Appl. Phys. A 72 (2001) 167.
[3] Y. Tsushio, E. Akiba, J. Alloys Comp. 269 (1998) 219.
[4] Y. Tsushio, P. Tessier, H. Enoki, E. Akiba, J. Alloys Comp. 280 (1998) 262.
[5] H. Oesterreicher, K. Ensslen, A. Kerlin, E. Bucher, Mater. Res. Bull. 15 (1980) 275.
[6] H. Oesterreicher, H. Bittner, J. Less-Common Met. 73 (1980) 339.
[7] T. Kohno, H. Yoshida, F. Kawashima, T. Inaba, I. Sakai, M. Yamamoto, M. Kanda, J. Alloys Comp. 311 (2000) L5.
[8] N. Terashita, K. Kobayashi, T. Sasai, E. Akiba, J. Alloys Comp. 327 (2001) 275.
[9] C. Geibel, U. Klinger, M. Weiden, B. Buschinger, F. Steglich, Phys. B 237–238 (1997) 202.
[10] K. Kadir, D. Noréus, I. Yamashita, J. Alloys Comp. 345 (2002) 140.
[11] K. Aono, S. Orimo, H. Fujii, J. Alloys Comp. 309 (2000) L1.
[12] M. Latroche, V. Paul-Boncour, A. Percheron-Guégan, J.-C. Achard, J. Less-Common Met. 161 (1990) L27.
[13] J.J. Reilly, R.H. Wiswall Jr., Inorg. Chem. 7 (1968) 2254–2256.
[14] K. Aoki, K. Shirakawa, T. Masumoto, Sci. Rep. Res. Inst. Tohoku Univ. Ser. A 32 (1985) 239.
[15] K. Aoki, T. Yamamoto, T. Masumoto, Sci. Rep. Res. Inst. Tohoku Univ. Ser. A 33 (1986) 163.
[16] K. Aoki, T. Yamamoto, T. Masumoto, Scripta Metall. 21 (1987) 27.
[17] M. Latroche, V.P. Boncour, A. Percheron-Guégan, Z. Phys. Chem. Bd. 179 (1993) 261.
[18] K. Suzuki, X. Lin, J. Alloys Comp. 193 (1993) 7.